Uroporphyrinogen Decarboxylase Structural Mutant (Gly^{281} → Glu) in a Case of Porphyria

HUBERT DE VERNEUIL, BERNARD GRANDCHAMP, CAROLE BEAUMONT, CHRISTIANE PICAT, YVES NORDMANN*

Uroporphyrinogen decarboxylase deficiency in man is responsible for familial porphyria cutanea tarda and hepatoerythropoietic porphyria. A recent study of a family with hepatoerythropoietic porphyria showed that the enzyme defect resulted from rapid degradation of the protein in vivo. Cloning and sequencing of a complementary DNA for the mutated gene revealed that the mutation was due to the replacement of a glycine residue by a glutamic acid residue at position 281. This base change leads to a protein that is very rapidly degraded in the presence of cell lysate. Characterization of the mutation will allow comparison of this defect in a homozygous patient with defects in other patients with familial porphyria cutanea tarda.

HEPATOERYTHROPOIETIC PORphyria (HEP) is a severe form of cutaneous porphyria that occurs early in infancy and is characterized clinically by photosensitivity, bullae, erosions, hypertrichosis, and red-colored urine (*1*). The patients have decreased uroporphyrinogen (Uro) decarboxylase activity in erythrocytes, fibroblasts, and lymphocytes (*2–4*). Family studies indicate that the patients are homozygous and their parents heterozygous for the same gene defect. We have recently investigated the basic molecular mechanism causing Uro decarboxylase deficiency in two patients with HEP (*5*). The enzyme defect in this family is accounted for by a rapid degradation of the protein in vivo.

The molecular cloning of normal human Uro decarboxylase complementary DNA (cDNA) has been reported, and the protein sequence has been deduced from the cDNA sequence (*6*). We have now cloned a DNA complementary to Uro decarboxylase messenger RNA extracted from a lymphoblastoid cell line of one of our two patients and sequenced this cDNA to determine the mutation responsible for the enzyme defect. Three overlapping clones covering the entire coding sequence except the two first codons have been isolated and sequenced. Comparison between the normal and mutated sequence revealed that they are identical except for four point mutations (Fig. 1A): (i) a T to C change at nucleotide 87 (relative to the 5′ end of pUD3) (*6*), (ii) an A to G change at nucleotide 325, (iii) a G to A change at nucleotide 860, and (iv) a T to C change at position 931.

The first and fourth substitutions, at positions 87 (GCT→GCC) and 931 (TTG→CTG), are silent polymorphisms. The second substitution, at position 325 (AGC→GGC, Ser→Gly; codon 103), has been observed previously and constitutes an established DNA polymorphism. Therefore the only significant sequence change in the Uro decarboxylase cDNA from our patient is the point mutation G→A at position 860, leading to a Gly (GGG) to Glu (GAG) change in the amino acid sequence (position 281). We investigated the effect of the mutation on the hydropathicity of the sequence (Fig. 1B). This revealed a drastic effect of the Gly to Glu mutation in codon 281. By contrast, the Ser to Gly mutation in codon 103 had no effect.

To confirm that the mutation 860 was not a cloning artifact but really led to the synthesis of an unstable protein, we used an in vitro transcription-translation system (Fig. 2A) that enabled us to produce two

H. de Verneuil, B. Grandchamp, C. Beaumont, Y. Nordmann, Faculty of Medicine X. Bichat, Department of Biochemistry, Hospital Louis Mourier, Colombes, France.
C. Picat, Institut National de la Santé et de la Recherche Médicale, U. 160, Hospital Beaujon, Clichy, France.

*To whom correspondence should be addressed.

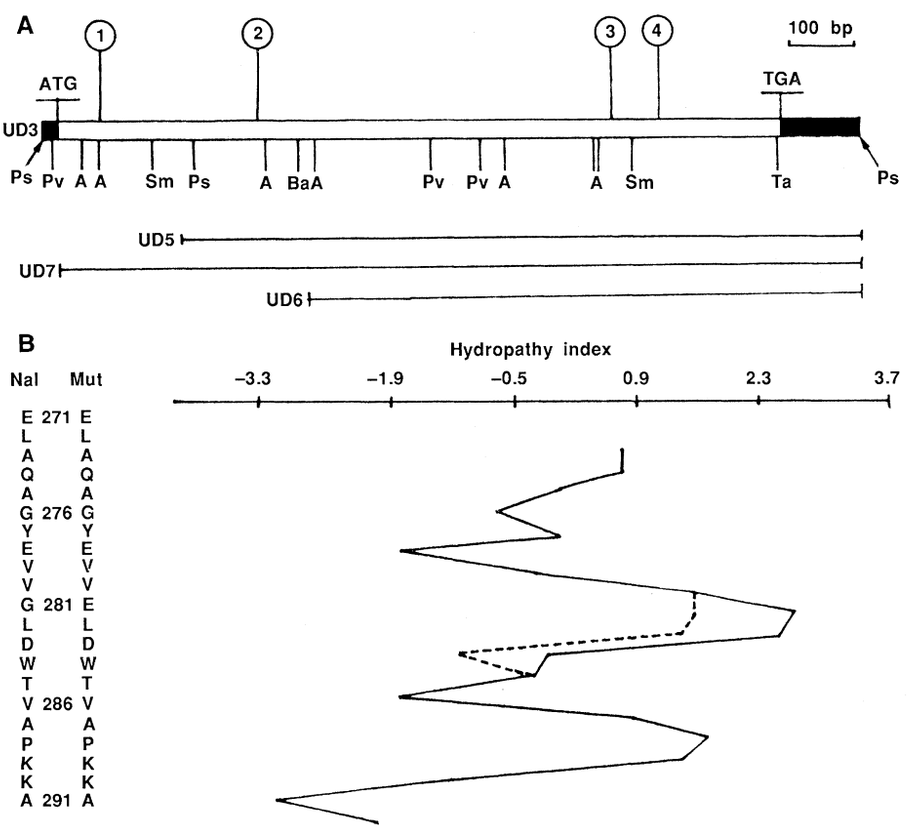

Fig. 1. Comparison of normal and mutated cDNA sequences. (A) The top line is a restriction map for the full-length cDNA UD3 [see (*6*) for the sequence]. The two arrows represent Pst I cloning sites. The translation initiation codon (ATG) and stop codon (TGA) are indicated. UD5, UD6, and UD7 represent the three clones isolated from the mutated cDNA library. Four point mutations, labeled 1, 2, 3, and 4 were found at positions 87, 325, 860, and 931, respectively. The restriction enzymes are A, Alu I; Ba, Bam HI; Ps, Pst I; Pv, Pvu II; Sm, Sma I; and Ta, Taq I. Double-stranded DNA complementary to polyadenylated RNA was synthesized as described by Gubler and Hoffman (*10*). The cDNA's longer than 500 bp were purified by high-performance liquid chromatography (LKB TSK G 4000-SW column). An oligo(dT)-primed cDNA library was then constructed in PBR322 by the homopolymeric tailing method. The 1020-bp Pst I–Pst I fragment of UD3 was used to screen the library. Three positive clones (UD5, UD6, and UD7) were digested with various restriction enzymes. The fragments were subcloned into the M13 sequencing vectors mp 10 and mp 11 and sequenced by the dideoxy chain–termination method. (B) Hydropathicity profile of a stretch of Uro decarboxylase protein (from codon 271 to 291) either with (Mut; broken line) or without (Nal; solid line) the mutation in codon 281. A computer program for the algorithm described by Kyte and Doolittle (*11*) was used to display the modification of the hydropathicity of the protein with a window of three amino acids.

proteins that differed only by the amino acid at position 281. Both cDNA's expressed in this in vitro system yielded a polypeptide product that had the same molecular weight as the protein in vivo and was specifically immunoprecipitated by a specific antibody to Uro decarboxylase. The two polypeptide products were very stable in the in vitro translation system (no significant degradation was observed for 8 hours at 37°C). However, the cDNA with the G to A mutation at nucleotide 860 yielded a protein that was very rapidly degraded in the presence of cell lysate (Fig. 2B). This result demonstrates that the Uro decarboxylase deficiency in this family is due to the mutation at nucleotide 860.

We used the technique recently developed by Myers *et al.* (*7*) to characterize the mutation in the cDNA. Two antisense RNA probes of different lengths (Fig. 3) were synthesized in the presence of [^{32}P]UTP. When either of these probes was annealed to the homologous wild-type cDNA fragment and then digested with ribonuclease A, a single full-length RNA fragment of 850 or 565 nucleotides was observed. In contrast, when the probes were annealed with the mutated cDNA, an RNA-DNA duplex containing a C-A mismatch at position 860 was created, and then two bands were observed after ribonuclease A digestion (370- and 480-nucleotide fragments for the 850-nucleotide probe; 370- and 195-nucleotide fragments for the 565-nucleotide probe). The sizes of the RNA fragments and the use of two probes of different lengths indicated that the cleavage occurred at the expected mismatch. The G to A mutation at position 860 introduces an Alu I site (AGCT) and could, theoretically, be identified by analysis of the restriction fragment lengths. This new restriction site has effectively been found on the cloned cDNA; a double digestion with the enzymes Alu I (AGCT) and Taq I (TCGA) led to the generation of a 270–base pair (bp) fragment for the normal UD3 cDNA and a 250-bp fragment for the mutated cDNA (see Fig. 1A for the position of restriction sites). However, the very high frequency of cutting with Alu I prevented the use of this enzyme for the direct detection of the point mutation in genomic DNA.

Since HEP may represent a homozygous form of familial porphyria cutanea tarda (PCT) (*2*–*4*), our characterization of the mutant gene responsible for two cases of HEP in a family will allow us to study the mutations in patients with familial PCT. The mutation we found may be common to other families with familial PCT or may represent a unique case of Uro decarboxylase defect. Detection of the single base substitution can be assayed by two methods: use of synthetic oligonucleotides complementary to wild-type and mutated sequences (*8*) or ribonuclease cleavage analysis on total genomic DNA (*7*) or RNA (*9*).

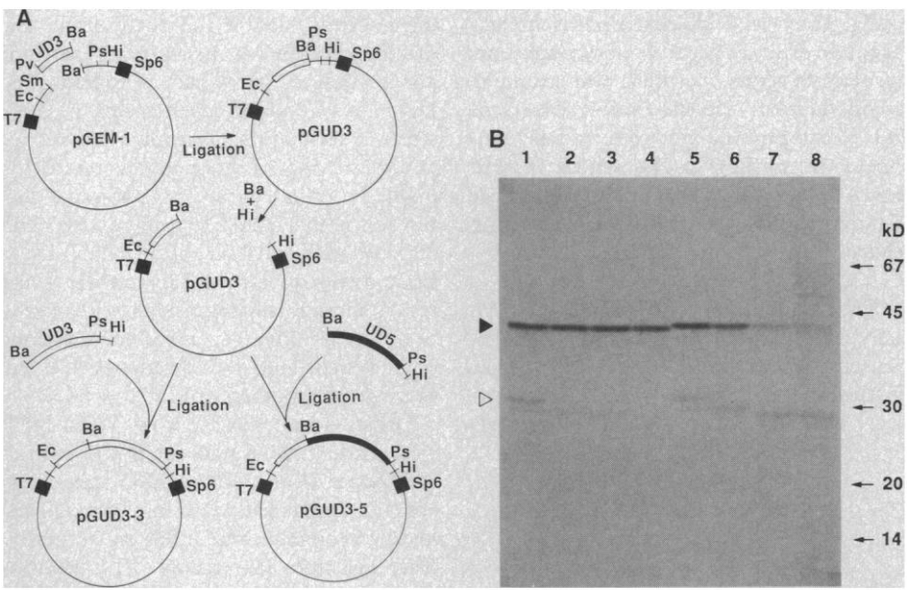

Fig. 2. Normal and mutated Uro decarboxylase proteins synthesized in an in vitro transcription-translation system. (A) Construction of transcription clones. Uro decarboxylase cDNA sequences were introduced in a two-step procedure into the transcription plasmid pGEM-1 (Riboprobe Gemini, Promega Biotec). Normal Uro decarboxylase sequences (UD3) are denoted by open boxes; mutated sequences (UD5) are denoted by solid boxes; T7 and Sp6 promoters are represented by solid squares. The restriction enzymes are Ba, Bam HI; Ec, Eco RI; Hi, Hind III; Ps, Pst I; Pv, Pvu II; and Sm, Sma I. The 372-bp Pvu II–Bam HI fragment of UD3 was subcloned in the polylinker of pGEM-1 to yield pGUD3. This plasmid was then digested with Bam HI and Hind III to insert the 870-bp Bam HI–Pst I fragment of UD3 or UD5 (containing a Hind III linker at the Pst I end) to yield pGUD3-3 and pGUD3-5, respectively. (B) Autoradiograph of a sodium dodecyl sulfate–polyacrylamide gel electrophoresis of proteins translated in vitro from synthetic mRNA's. Normal (lanes 1 to 4) and mutated (lanes 5 to 8) Uro decarboxylase proteins (closed arrowhead) were found with the expected molecular weight. Another faint band with a lower molecular weight (open arrowhead) was also found. It arose from the use of an internal start site with a consensus-like sequence at Met 100 (*6*). Portions (2 μl) of the translation mixture were incubated at 37°C for 0 (lanes 1 and 5), 4 (lanes 2 and 6), 8 (lanes 3 and 7), and 24 hours (lanes 4 and 8) in the presence of 10 μl of sonicated lymphocyte lysate (2.5 mg/ml). The ^{14}C-labeled protein markers are bovine serum albumin, ovalbumin, carbonic anhydrase, soybean trypsin inhibitor, and lactalbumin. Transcripts were synthesized from Hind III–linearized pGUD3-3 and pGUD3-5 by using the T7 promoter as described by Krieg and Melton (*12*) and translated in a micrococcal nuclease–treated rabbit reticulocyte system (*13*) in the presence of [^{35}S]methionine. Translation products were analyzed by sodium dodecyl sulfate–polyacrylamide gel electrophoresis by the method of Laemmli (*14*). The gel was fixed with 10% acetic acid, dried, and autoradiographed (4 hours).

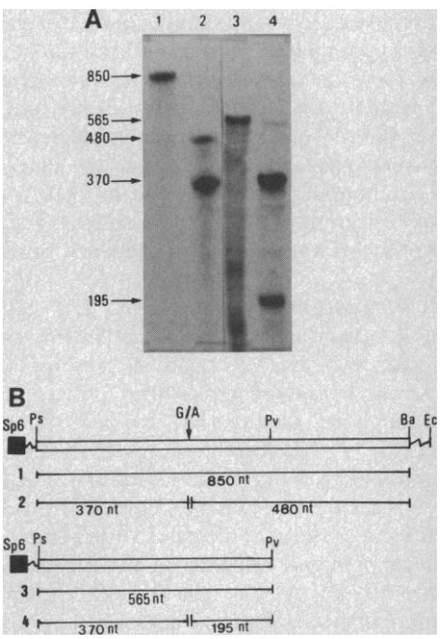

Fig. 3. Ribonuclease cleavage analysis of normal and mutated sequences. (A) Autoradiograph of the ribonuclease digestion products obtained with normal (lanes 1 and 3) or mutated sequences (lanes 2 and 4) hybridized either with the 850-nucleotide probe (lanes 1 and 2) or with the 565-nucleotide probe (lanes 3 and 4). (B) Diagram of the different fragments obtained. The arrow (G/A) indicates the position of the mutation with a G nucleotide with the normal sequence and an A with the mutated sequence. Radioactive antisense RNA probes were transcribed from the pGEM-1 vector containing the 850-bp Pst I–Bam HI fragment of UD3. The plasmid was linearized at the Eco RI site (850-nucleotide probe) or at the Pvu II site (565-nucleotide probe). Synthesis was done with the Sp6 promoter in the presence of [^{32}P]UTP (*10*) (specific activity, 40 Ci/mmol). Conditions of hybridization and digestion with ribonuclease A were the same as described by Myers *et al.* (*7*).

REFERENCES AND NOTES

1. A. Kappas, S. Sassa, K. E. Anderson, *The Metabolic Basis of Inherited Disease*, J. B. Stanbury, J. B. Wyngaarden, D. S. Fredrickson, J. L. Goldstein, M. S. Brown, Eds. (McGraw-Hill, New York, 1983), p. 1301.
2. G. H. Elder *et al.*, *Lancet* **1981-I**, 916 (1981).
3. H. de Verneuil *et al.*, *Am. J. Hum. Genet.* **36**, 613 (1984).
4. P. Lazaro *et al.*, *Br. J. Dermatol.* **110**, 613 (1984).
5. H. de Verneuil *et al.*, *J. Clin. Invest.* **77**, 431 (1986).
6. P. H. Roméo *et al.*, *J. Biol. Chem.* **261**, 9825 (1986).
7. R. M. Myers, Z. Larin, T. Maniatis, *Science* **230**, 1242 (1985).
8. M. Pirastu *et al.*, *N. Engl. J. Med.* **309**, 284 (1983); V. J. Kidd *et al.*, *Nature (London)* **304**, 230 (1983).
9. E. Winter, F. Yamamoto, C. Almoguera, M. Perucho, *Proc. Natl. Acad. Sci. U.S.A.* **82**, 7575 (1985).
10. U. Gubler and B. J. Hoffman, *Gene* **25**, 263 (1983).
11. J. Kyte and R. F. Doolittle, *J. Mol. Biol.* **157**, 105 (1982).
12. P. A. Krieg and D. A. Melton, *Nucleic Acids Res.* **12**, 7057 (1984).
13. H. R. Pelham and R. J. Jackson, *Eur. J. Biochem.* **67**, 247 (1976).
14. U. K. Laemmli, *Nature (London)* **227**, 680 (1970).
15. We thank P. H. Roméo and M. Goossens (INSERM U.91, Créteil, France) for donating pUD3 cDNA, J. Y. Picard and A. Kahn (INSERM U.129, Paris, France) for help with DNA sizing, H. Nicolas (INSERM U.73, Paris, France) for technical assistance in cell cultures, and C. Guyomard for assistance in the preparation of the manuscript. Supported in part by grant CRE 83.10.12 from the Institut National de la Santé et de la Recherche Médicale, by Caisse Nationale de l'Assurance Maladie des Travailleurs Salariés, and by Université Paris 7 (Faculté de Médecine X. Bichat).

7 July 1986; accepted 15 September 1986

The Brain Nucleus Locus Coeruleus: Restricted Afferent Control of a Broad Efferent Network

GARY ASTON-JONES, MATTHEW ENNIS, VINCENT A. PIERIBONE, W. THOMPSON NICKELL, MICHAEL T. SHIPLEY

Dense, focal injections of wheat germ agglutinin conjugated–horseradish peroxidase in the locus coeruleus of rats labeled afferent neurons in unexpectedly few brain regions. Major inputs emanate from only two nuclei—the paragigantocellularis and the prepositus hypoglossi, both in the rostral medulla. The dorsal cap of the paraventricular hypothalamic nucleus and the spinal intermediate gray are possible minor afferents to locus coeruleus. Other areas reported to project to locus coeruleus (for example, amygdala, nucleus tractus solitarius, and spinal dorsal horn) did not exhibit consistent retrograde labeling. Anterograde tracing and electrophysiologic experiments confirmed the absence of input to locus coeruleus from these areas, which instead terminate in targets adjacent to locus coeruleus. These findings redefine the anatomic organization of the locus coeruleus, and have implications for hypotheses concerning the functions of this noradrenergic brain nucleus.

THE LOCUS COERULEUS (LC) HAS attracted intense interest in the last two decades, largely because of its pervasive noradrenergic fiber projections throughout the central nervous system (CNS). A considerable body of evidence implicates this nucleus in global brain functions such as emotion and vigilance, as well as in the etiology of mental disorders such as depression and dementia of the Alzheimer type (*1, 2*). At the cellular level, perhaps more is known about the anatomical projections and postsynaptic effects of the LC than any other system in brain (*3*). Recent studies have also revealed a homogenous set of discharge properties for these cells and shown that specific behavioral and sensory events evoke concerted activity of LC neurons (*4, 5*; reviewed in *6*).

In contrast to this knowledge of the physiology, pharmacology, and efferent anatomy of the LC system, little is known about the neural inputs that regulate activity in this nucleus. Specification of the afferents that control LC discharge is critical to understanding the neural circuitry in which this system functions and, therefore, to generating hypotheses concerning its role in brain and behavioral processes.

In previous attempts to define inputs to rodent LC, injections of horseradish peroxidase (HRP) were used to label afferent neurons by retrograde transport. In the few studies of this type (*7*), many CNS structures were found to contain retrogradely labeled cells, but no functional pattern of afferent innervation emerged. Since these initial neuroanatomic studies were conducted, retrograde tracing techniques have improved substantially. In particular, recent methods employing the tracer wheat germ agglutinin–conjugated HRP (WGA-HRP), combined with the histochemical substrate tetramethylbenzidine (TMB), are many times more sensitive than techniques utilizing nonconjugated HRP as the tracer and diaminobenzidine as the substrate (as in the above studies) (*8*). Thus, we reexamined inputs to LC, taking advantage of the more sensitive techniques presently available; we anticipated that additional afferents to LC might be found. However, we found that the LC is innervated by only a few brain regions, with the bulk of afferents arising from two rostral medullary nuclei. These results substantially redefine the circuit relationships of this pervasive noradrenergic brain system and, therefore, have a direct bearing on hypotheses of LC function.

Fig. 1. LC injection site. Bright-field photomicrograph of a coronal section through LC of an experimental rat brain. WGA-HRP was iontophoresed into LC and tissue processed with TMB after a 24-hour survival period (*9, 11*). Note the dense deposit of tracer (black area) confined to the LC. Medial (fourth ventricle) is to the right and dorsal is at the top.

Dense, focal injections of WGA-HRP were made by iontophoresis from glass micropipettes (*9*) in adult, male Sprague-Dawley rats. Single cell recordings through the injection pipette were used to accurately place injections [for example, LC neurons were recognized by their distinctive waveform and responsiveness to sensory stimuli (*3, 10*)]. Eighteen to thirty-six hours after injection, brains were prepared for HRP histochemistry with TMB as the substrate (*11*).

Our conclusions are based on an analysis of injection sites centered unilaterally in the LC (33 cases) (Fig. 1). Neurons were considered retrogradely labeled if at least ten TMB reaction granules were visible within the Nissl-stained cell. Injections confined to

G. Aston-Jones, M. Ennis, V. A. Pieribone, Department of Biology, Washington Square Center for Neural Science, New York University, New York, NY 10003.
W. T. Nickell, Department of Cell Biology and Anatomy. University of Cincinnati, College of Medicine, Cincinnati, OH 45267.
M. T. Shipley, Departments of Cell Biology and Anatomy and Neurosurgery, University of Cincinnati, College of Medicine, Cincinnati, OH 45267.